

The Particle Flux Structure and the Search for a Flux-Expansion Divertor in TJ-II

Francisco CASTEJÓN^{1,2}, Antonio LÓPEZ-FRAGUAS¹,
Alfonso TARANCÓN^{2,3} and José L. VELASCO^{2,3}

¹*Laboratorio Nacional de Fusión-Asociación Euratom/Ciemat, Madrid 28040, Spain*

²*Instituto de Biocomputación y Física de Sistemas Complejos, Universidad de Zaragoza, Zaragoza 50009, Spain*

³*Departamento de Física Teórica, Universidad de Zaragoza, Zaragoza 50009, Spain*

(Received 16 November 2007 / Accepted 5 March 2008)

We explore the possibility of having a flux-expansion divertor in TJ-II. As a first step, the three-dimensional map of the particle flux has been obtained for two different plasma regimes using the code ISDEP, which computes the ion guiding-centre trajectories. We consider the particle trajectories rather than the field lines due to the fact that, in TJ-II, common ion orbits can separate from the field lines, and moreover the plasma electric field and the collisionality must be considered. We have chosen a configuration that presents flux expansion at given toroidal positions. We have estimated the heat and particle fluxes and checked that it is possible to reduce them strongly by intersecting the trajectories at a given zone of the space. Future studies, maybe including the creation of an ergodic zone, will determine the best strategy for intercepting the trajectories.

© 2008 The Japan Society of Plasma Science and Nuclear Fusion Research

Keywords: flux expansion, divertor, ion kinetic transport, Montecarlo method

DOI: 10.1585/pfr.3.S1009

1. Introduction and Motivation

The quest for the stellarator reactor needs a robust divertor concept to guarantee low plasma-wall interaction and power exhaust [1]. A good divertor concept should strongly reduce the particle and heat fluxes on the stellarator wall and concentrate this interaction in favourable zones. There, plates of a low- Z material may be located and additional pumping could be operative, in order to reduce the incoming of impurities. Additionally, the path of the recycled neutrals that are to enter the plasma must be large in the real space, and the plasma profiles should present a steep pressure gradient in the edge. Ideally, with these conditions the recycled neutrals cannot go back to the plasma centre, since they are ionized close to the edge and do not penetrate into the plasma core. The geometry of the divertor plates and the divertor chamber must be designed in such a way that the amount of delivered impurities is minimized.

The divertor programme in stellarators needs to consider a wide range of concepts due to the diverse possible configurations that are presently in operation and those that will appear in the future. In tokamaks, the divertor based on locating one or two X points inside the vacuum chamber has been demonstrated as a good solution.

As for stellarators, LHD presents the helical divertor concept. It is based in a natural ergodic zone of its magnetic configuration that rotates with the same law as the helical coils of the device [2]. This configuration ensures

that almost all the flux escaping from the plasma hits the divertor plates, instead of the vacuum chamber, due to the open field lines outside the last closed flux surface (LCFS). The island-based divertor is a promising concept, as has been demonstrated in W7-AS [3], where excellent results have been obtained. In this device, the plasma-wall interaction was strongly reduced and the High Density H mode was reached. This concept is suitable for the W7-X device, which will have a fixed robust magnetic configuration.

For these two former divertor concepts to work, it is necessary that the island positions and widths do not change substantially during plasma operation and, in this way, the topology of the helical and island divertor is not modified. There are several causes that can strongly change the topology during plasma-wall operation. The first one is that the magnetic configuration relies on the bootstrap current. This happens in the two stellarators projected in Oak-Ridge and Princeton, QPS (Quasi Poloidal Symmetric Stellarator, see for instance [4]) and NCSX (National Compact Stellarator Experiment, see e.g. [5]). Secondly, the magnetic topology can change in devices that present high flexibility in their rotational transform values, like TJ-II [6]. Finally, an increase of plasma pressure can change the equilibrium and create magnetic islands and ergodic areas in the plasma edge, strongly modifying the edge topology and the divertor structure.

In those cases, the flux expansion concept [7] could be a good candidate for the divertor. This concept is based on intercepting the particle and energy fluxes with plates

author's e-mail: francisco.castejon@ciemat.es

in an ergodic area of the plasma where the magnetic lines are well separated, so that the power flux onto the plates is small enough and the resulting neutrals and impurities can be pumped. The large flux expansion should also guarantee that the neutrals entering the plasma have to perform a large path, thus diminishing the probability that they go deep inside the device core.

There is not a canonical definition of flux expansion, therefore we introduce here one, $\mathcal{F} \equiv (d\rho/dr)^{-1}$, in order to quantify the effect. Here, $\rho = \sqrt{\psi/\psi_0}$ is the normalized radial coordinate, while ψ and ψ_0 are the magnetic toroidal fluxes through the local and the last closed magnetic surfaces; r is the physical distance to the magnetic axis.

There is no experience about the performance of this kind of divertor in any magnetic confinement device. Nevertheless, it has been recently pointed that H mode was not only reached at JET by a usual X-point divertor, but also by locating the X point outside the vacuum chamber (see [8] and references therein). This transforms the divertor configuration into a limiter configuration with flux expansion. The results of JET have therefore shown that the flux expansion divertor can work and accomplish the same functions as a conventional divertor. Moreover, in the JET case, this way of operation of the device allows to increase the plasma volume and, hence, to improve the confinement. This is a first indication that a divertor based on the same properties could also work for stellarators.

The remainder of this paper is organized as follows. The TJ-II characteristics relevant for the plasma-wall interaction are developed in Section 2. Section 3 is devoted to the description of ISDEP code and to show the characteristics of the two plasma regimes chosen to perform these simulations. The selected configuration is described in Section 4 and the results of the calculations are shown in Section 5. Finally, the conclusions and future work come in Section 6.

2. The Specific TJ-II Characteristics

TJ-II presents specific plasma-wall interaction issues. Part of its vacuum chamber has a groove that surrounds the central conductor and acts as a helical limiter. Due to its magnetic configuration, the groove is the preferred zone for the escaping particles to strike, as will be discussed in Section 5. Since the groove is physically close to the centre of the device (about 12 - 14 cm, depending on the configuration) one should try to diminish this flux by intersecting the particle trajectories far from that position. Otherwise it is guaranteed that a large fraction of the recycled neutrals will return to the plasma and reach its inner part.

We have found several magnetic configurations that are suitable for this divertor concept, since they have plasma zones where the density of magnetic surfaces is especially low, i.e., where the flux expansion is large enough. The point is to look for a position in which the efficiency of the divertor is maximum (i.e. intersects a large fraction

of the heat and particle fluxes) and to try to make this requirement compatible with a low enough heat flux on the plates.

No natural ergodic zones appear outside the LCFS in TJ-II. This outermost flux surface is therefore defined by the groove, which follows the same winding law around the central conductor as the magnetic axis. Therefore, a second phase of this work may imply the creation of this ergodic zone by introducing extra coils that create a resonant magnetic field.

3. ISDEP Code and the Chosen Plasma Conditions

Previous calculations performed to explore the flux expansion concept divertor in NCSX [7] followed magnetic field line trajectories including a diffusion coefficient of about 1 ms^{-2} , of the order of the one experimentally measured. This approach happens to be valid for devices where the particle trajectories do not separate very much from the field lines. This is not fulfilled in TJ-II [9] due to the large drifts appearing in this device, and the particle trajectories must be followed to estimate the fluxes.

ISDEP (Integrator of Stochastic Differential Equations in Plasmas) [10], is a Montecarlo code that follows ion guiding-centre trajectories considering a given electrostatic potential profile and ion-ion as well as ion-electron Coulomb collisions [11]. The advantage of calculating the heat and particle fluxes in this way is that no assumptions on the diffusive nature of transport and on the size of the orbits are necessary (these assumptions are mandatory in the customary neoclassical estimations). Furthermore, since it is not necessary to take averages on the magnetic surfaces, a three-dimensional map of the fluxes can be obtained, which is crucial for this study. This code has been used in the present work to study the ion collisional flux properties in the chosen magnetic configuration and various plasma regimes.

Obviously, the quantitative results will depend on the plasma characteristics, namely the collisionality and the electrostatic potential. Nevertheless, we expect our results on the divertor effect to hold in a range of plasma parameters, especially in the high β regime. In order to check this, two characteristic (and very different) plasma regimes have been chosen in this work. The plasma profiles are shown in Fig. 1 as a function of the effective radius ρ .

The plasma parameters used in our simulations are taken similar to those obtained experimentally in the two regimes. The density and electron temperature are obtained from Thomson-Scattering measurements [12]: the error bars are of the order of 10% for the electron temperature and 5% for the density. The ion temperature profiles are taken from the CX-NPA diagnostic [13], in shot to shot experiments. The typical error bars for these measurements are again about 10%. Finally, the electrostatic potential comes from HIBP measurements [14].

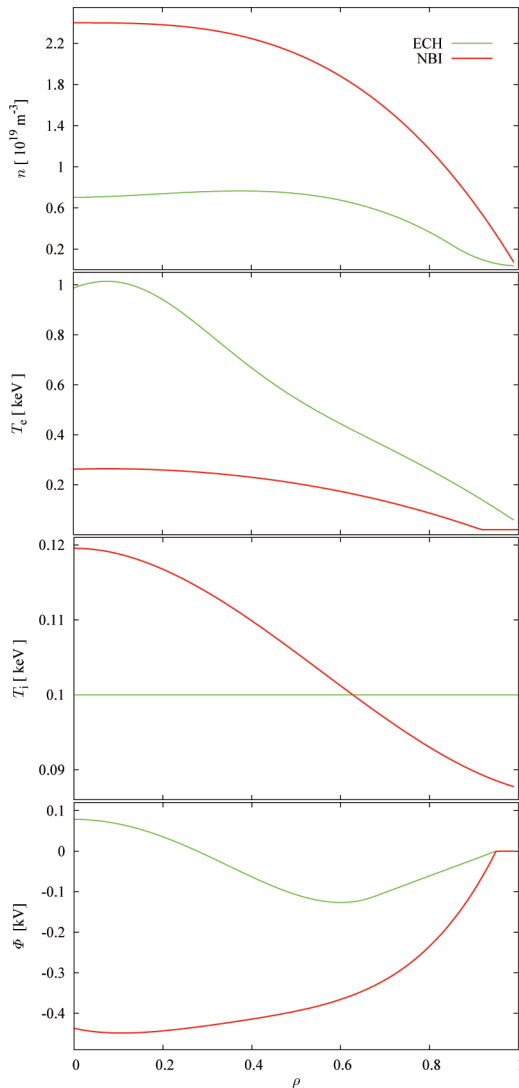


Fig. 1 Radial plasma profiles as functions of the normalized radius in the two regimes (ECH: green; NBI: red). From top to bottom: density, electron temperature, ion temperature and plasma electrostatic potential. These profiles are taken similar to the experimental ones.

In green, we show a low density, low collisional ECRH (electron cyclotron resonance heating) plasma, whose profiles are similar to those shown in [12]. It is characterized by a positive electric field in the core, according to the electron root [15]. The ion temperature profile is almost flat within the error bars, and that of the electron temperature is peaked. The density profile is hollow. The chosen ECRH case corresponds actually to an intermediate plasma density and the electrostatic potential is non-monotonic: it shows a transition from the electron root (positive electric potential) in the centre of the device to the ion root (negative electric potential) in the edge. Therefore, the electrostatic potential presents a minimum at $\rho = 0.6$, which implies that the ions tend to accumulate close to this zone. The almost flat ion temperature profile was found in [16] and was attributed to the existence

of a non-diffusive ion transport. This hypothesis has been confirmed by recent calculations with ISDEP code [17].

In red, we plot an NBI (neutral beam injection) plasma. The density is high and the electron temperature is low, with parabolic profiles, as in [18]. In this case, the ion temperature is not flat, but presents a steeper gradient than the ECH case. The potential corresponds to a plasma which is in the ion root along the minor radius. The electrostatic potential is thus monotonic (except a small region close to the centre) and negative, as corresponds to the ion root. This potential tends to enhance the ion confinement, which will have strong consequences on the flux structure.

4. The Chosen Configuration

One of the main properties of TJ-II heliac is its flexibility. It is possible to change the plasma size and shape as well as the rotational transform (TJ-II is an almost shearless device) by changing the currents that circulate by the two coils of the central conductor. Specifically, the high rotational transform configurations present a more indented shape and, hence, a larger flux expansion at some toroidal and poloidal angles.

After studying several magnetic configurations, we have chosen the 100_68_91 (the numbers stand for the currents that circulate by the coils), which presents a large flux expansion at given toroidal positions. The average plasma minor radius is $a = 0.2$ m and the rotational transform in the edge is $\iota/2\pi = 1.825$. In this magnetic configuration, similarly to the majority of those of TJ-II, a large fraction of the particle fluxes strike the groove, as will be shown in Section 5. Therefore, the neutrals coming from the wall appear very close to the plasma bulk, as it has been commented above. Hence, the main goal of the divertor designed for TJ-II is to diminish as much as possible the fluxes that are directed to the groove. In this way the plasma-wall interaction would concentrate in a much more favourable region, far from the plasma centre. Figure 2 shows several Poincaré maps of the field lines of the chosen configuration (the sections have been rotated poloidally an angle four times the toroidal position for a better comparison). It is possible to appreciate that the maximum flux expansion happens for a toroidal angle around $\phi = \pi/4$ (and, of course, also around $\phi = 3\pi/4, 5\pi/4$ and $7\pi/4$, since TJ-II is a four-period device). At this region, the coronas are wider, i.e., the magnetic surfaces are more separated (this effect is quantified below). Fortunately, the zone with large flux expansion lays on a wide range around these angles. This gives us quite a lot freedom in our optimization task.

Figure 3 shows a particular toroidal section, together with a sketch of the wall of the vacuum chamber. The distance from the magnetic axis to the groove is about 12 cm in this configuration, and only a thin layer of plasma of about 5 cm separates the edge and the plasma bulk (distance in real space between the axis and the LCFS in the groove poloidal position). Nevertheless, this layer is about

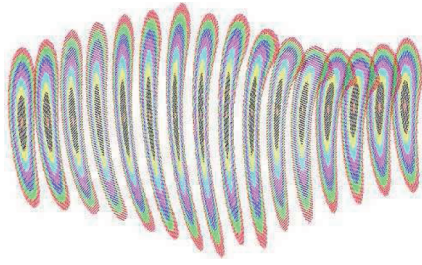


Fig. 2 Plasma toroidal sections (rotated poloidally an angle 4ϕ so that it can be compared). Each color corresponds to a corona of width $\Delta\rho = 0.1$. The last corona is $0.8 < \rho < 0.9$. The surfaces in the ends lay in $\phi = 0$ (left) and $\phi = \pi/2$ (right).

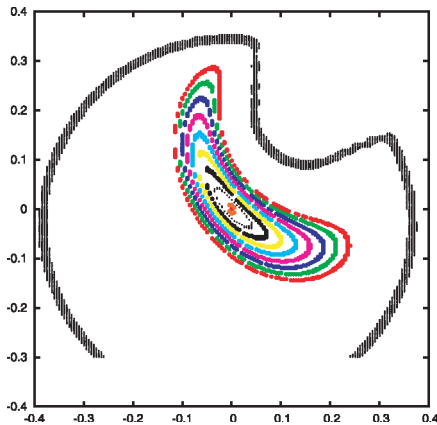


Fig. 3 Magnetic surfaces at $\phi \approx \pi/6$ and sketch of the wall of the vacuum chamber.

25 cm in the poloidal angle corresponding to one of the extremes of the “bean”. Therefore, if the plasma-wall interaction can be concentrated at the zone where the flux expansion is maximum (about a factor 5 higher), the particle flux onto the groove will be strongly reduced. The amount of neutrals that enter the plasma bulk will also decrease since the physical distance is multiplied by a factor 5.

5. Design and Results

In order to search for the optimal position of the plates, we have performed a map of the ion flux on several magnetic surfaces and at different toroidal and poloidal angles. Since TJ-II is a four-field-period device, our results are (statistically) identical on each period. Therefore, we will consider all of them in our calculations and show them averaged in the first period. This has been done by adding the values of the fluxes at equivalent toroidal angles. We have accomplished our task defining our plates as the locus of points such that:

$$\rho_0 < \rho, \quad (1)$$

$$\frac{2\pi}{N_\phi} i < \phi < \frac{2\pi}{N_\phi} (i + 1), \quad (2)$$

$$\frac{2\pi}{N_\theta} j < \theta < \frac{2\pi}{N_\theta} (j + 1). \quad (3)$$

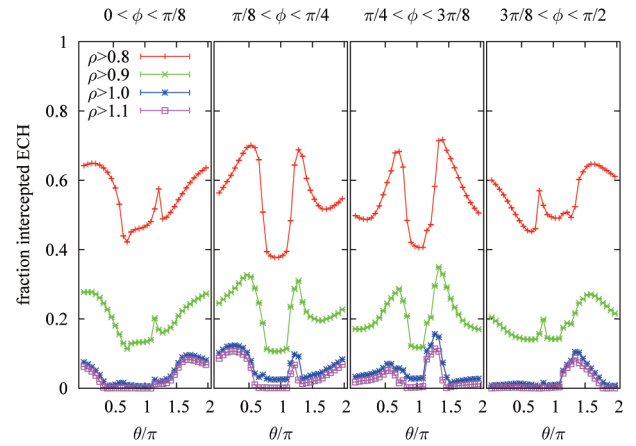


Fig. 4 Proportion of ions intercepted by the toroidally extended plate as a function of the angular position of the plate for the ECH plasma. The four toroidal plates cover a single period.

By setting $N_\phi = 16$ (four ϕ -intervals in a period) and $N_\theta = 32$, we have 128 plates defined in each period, corresponding to 512 different plates in TJ-II. An sketch of one ensemble of them will be shown in Fig. 6. Note that these plates are tangent to the magnetic surface ρ_0 , and intersect the field lines in $\rho > \rho_0$ of an angular region.

We follow a large number of ion trajectories and study the individual effect of each plate on the particle flux. More precisely, in Fig. 4 we show, for the ECH plasma, the fraction of the trajectories that would be intercepted by each plate in the case that this plate were the only one in our device. Note that the contributions of two plates cannot be directly added, since they may partly shadow each other. Studying the structures that appear in the flux (see Fig. 4) it is possible to infer the optimum positions where a plate can be more effective. We will be interested in plates in the outer region of the plasma, where $\rho > 1.0$, for an acceptable interaction of the plate with the hot plasma. In such radial positions, the plates defined by $\theta \approx 3\pi/2$ for $\pi/4 < \phi < 3\pi/8$ and $3\pi/8 < \phi < \pi/2$ look promising, since 10% of all the particles would be intercepted by each of them. Considering the mirror images of these plates in the other three periods (although, as we know, their contributions do not simply add up), one could expect to concentrate a great proportion of the plasma-wall interaction in these plates. Note that our choice is not the optimal on intercepting particles, but it is the best that makes it far from the groove.

Figure 5 shows the same quantity for the case of the NBI plasma. Here, the radial electric field clearly improves the confinement, especially in the plasma edge. One of the consequences is that each ion has more probability of being intercepted by each plate, since it performs more toroidal turns around TJ-II before leaving the plasma. This fact explains why the fluxes are larger in this case. Our former proposal of divertor configuration still seems one of

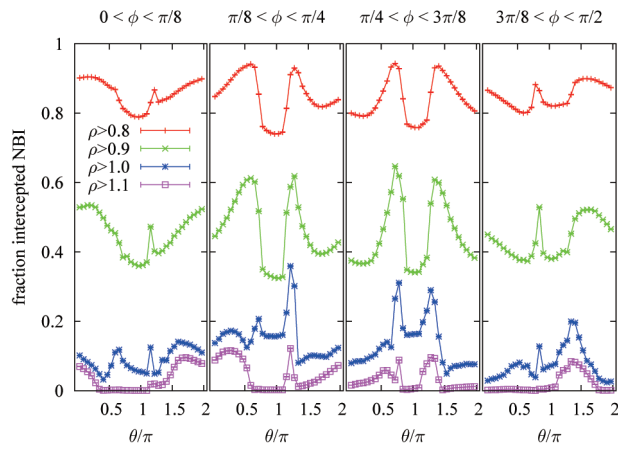


Fig. 5 Same as Fig. 4 for the NBI plasma.

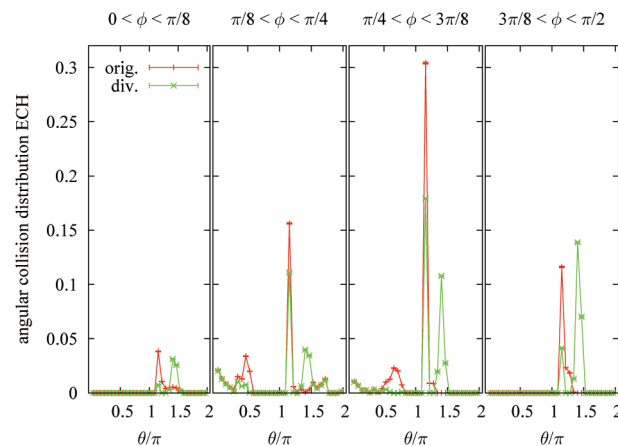

 Fig. 6 Tentative location of plates in the flux expansion divertor in the TJ-II Flexible Helicoid. The $0.9 < \rho < 1.0$ surfaces are plotted in black, and the plates in red.


Fig. 7 Angular distribution of the collisions with the vacuum chamber and the plates for the ECH plasma with and without divertor.

the best possible. These are good news, since one would desire a divertor design valid for a wide range of plasma parameters. Looking at both figures, our first tentative design will be plates located at $\rho > 1.0$, $11\pi/8 < \theta < 23\pi/16$ along all the toroidal angle. This configuration is sketched in Fig. 6.

In the ECH case, our plates intercept about half the particles in the plasma. This includes ions that end their trajectories in the groove and ions that do not. The original and the modified angular distributions of trajectory ends

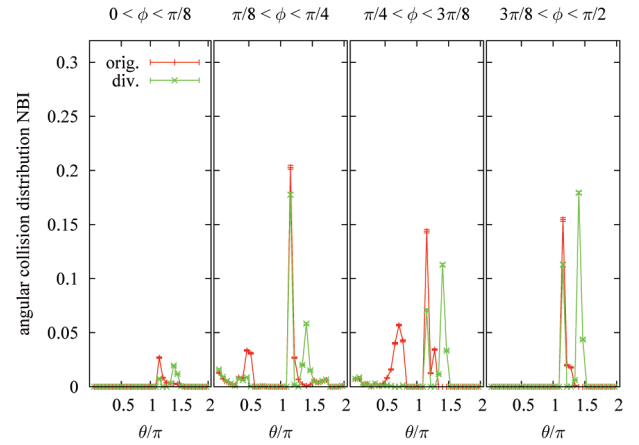


Fig. 8 Same as Fig. 7 for the NBI plasma.

are shown in Fig. 7. The high original peaks correspond to collisions with the groove, which in usual operation represent around 60% of the collisions with the vacuum chamber. The effect of our plates is to diminish this quantity so that it is around 35%, about half the proportion existing before. New peaks appear, corresponding to the location of our plates. This means that we have concentrated a great part of the plasma-wall interaction on the divertor plates.

In the case of the NBI plasma, see Fig. 8, the same effect still exists. The proportion of the total trajectories that are intercepted is about 63%. Nevertheless, from about 50% of ions colliding with the groove, this amount get reduced to about 35%.

6. Conclusions and Future Work

We have found a promising family of configurations suitable for having a flux expansion divertor in TJ-II. Those configurations are characterized by presenting a very indented plasma shape and for having high rotational transform value (above 1.5). The particle collisional flux maps are characterized by presenting strong poloidal asymmetries, showing a high value in the poloidal position corresponding to one of the extremes of the "bean". This particular characteristic of TJ-II ensures that locating the divertor plates close to the position where these fluxes are maximum will ensure that the particle and heat fluxes onto the groove of the vacuum chamber are strongly diminished.

This kind of magnetic configurations has the property that the flux expansion is maximum in a region where the main part of the particle flux that goes onto the groove passes through. Therefore, one may minimize at the same time the flux onto the groove and onto the plates. Due to the TJ-II configuration characteristics, this effect is especially beneficial because we move the main plasma wall interaction to a zone much farther from the plasma bulk: the physical distance is enhanced by a factor 5.

The beneficial effect of the divertor is larger in the NBI regime despite of the fact that this case presents a shorter mean free path, because the structure of electrostatic poten-

tial ensures that a large fraction of particles is intercepted. The next step of this work is to optimize the design of the divertor plates in order to interrupt as much as possible the flux onto the groove. This optimization process could force us to design toroidally and poloidally extended plates.

It may be also necessary to create an ergodic zone in order to minimize the particle and heat fluxes on the plates. The plasma pressure itself could be the cause of the appearance of this ergodic zone (the 5/9 resonance is close to the edge in this configuration). It is also possible to create the ergodization by introducing some perturbative coils.

Before assessing the feasibility of this construction, new flux calculations with the ergodic zone are mandatory. For this last phase of calculation, the effect of turbulence on particle trajectories must be included. Once the flux on the divertor plate is estimated, including the field ergodization effect, and before starting the engineering assessment of the coils and the divertor plates, it will be necessary to calculate the outgasing coming from the plates. EIRENE code can be adapted to this structure to allow us to study the neutral transport. Experiments are also foreseen in TJ-II to benchmark all these theoretical results.

Acknowledgments

The authors are grateful to Luis Antonio Fernández and Víctor Martín-Mayor for discussions. They also acknowledge partial financial support from European Commission through contracts, EGEE-II-031688 and int.eu.grid 03185. J L Velasco is a DGA (Aragon, Spain) fellow. The calculations presented in this work have been performed using grid computing techniques on the Fusion Virtual Organization of EGEE-II (Enabling Grids for E-

sciencE) project and the Cluster at BIFI.

- [1] R. König *et al.*, Plasma Phys. Control. Fusion **44**, 2365 (2002).
- [2] N. Ohya *et al.*, Nucl. Fusion **34**, 387 (1994).
- [3] Y. Feng *et al.*, Nucl. Fusion **46**, 807 (2006).
- [4] D.A. Spong, S.P. Hirshman, J.F. Lyon, L.A. Berry and D.J. Strickler, Nucl. Fusion **45**, 918 (2005).
- [5] A.H. Reiman, G. Fu, S. Hirshman, L. Ku, D. Monticello, *et al.*, Plasma Phys. Control. Fusion **41**, B273 (1999).
- [6] C. Alejandre *et al.*, Fusion Technol. **17**, 131 (1990).
- [7] R. Maingi, "Magnetic Field Line Tracing Calculations for Conceptual PFC Design in NCSX, and possibilities for a divertor design collaboration", 33th EPS Conference on Plasma Phys. Control. Fusion, Roma (2006).
- [8] P.H. Rebut, Plasma Phys. Control. Fusion **48**, B1 (2006).
- [9] F. Castejón *et al.*, Fusion Sci. Technol. **50**, 412 (2006).
- [10] F. Castejón *et al.*, Plasma Phys. Control. Fusion **49**, 753 (2007).
- [11] A. Boozer and G. Kuo-Petravic, Plasma Phys. **24**, 851 (1981).
- [12] J. Herranz *et al.*, Phys. Rev. Lett. **85**, 4715 (2000).
- [13] R. Balbín *et al.*, "On the ion confinement and neutral density at the plasma center of TJ-II stellarator", 30th Conference on Controlled Fusion and Plasma Physics. St. Petersburg, Russia, (2003). European Conference Abstracts, Vol 27A, (2003).
- [14] Melnikov *et al.*, Fusion Sci. Technol. **46**, 299 (2004).
- [15] M. Yokohama *et al.*, Nucl. Fusion **47**, 1213 (2007).
- [16] J.M. Fontdecaba *et al.*, Fusion Sci. Technol. Fusion **46**, 271 (2004).
- [17] J.L. Velasco *et al.*, Nucl. Fusion **48**, 065008 (2008).
- [18] R. Balbín *et al.*, "Ion Temperature Profiles During NBI Plasma Heating on the TJ-II Stellarator", 15th International Stellarator Workshop, Madrid (2005).